RESEARCH PAPER

A ratiometric fluorescent sensor for tetracyclines detection in meat based on pH-dependence of targets with lanthanum-doped carbon dots as probes

Ya Jie Fan[1] · Ming Su[1] · Yu-E. Shi[1] · Xiao Tong Liu[1] · Shi Gang Shen[1] · Jiang Xue Dong[1]

Abstract

Although some ratiometric fluorescent sensors have been reported to detect tetracyclines, most of ratiometric fluorescent sensors were established based on europium ion with a narrow linear range. In this work, a ratiometric fluorescent sensor for tetracyclines detection was established based on the dual-emission lanthanum-doped carbon dots (La-CDs) as probes combining with the characteristic pH-response of tetracyclines. The fluorescence intensity of tetracyclines will be enhanced in high pH, and the emission peak of tetracyclines overlapped with the peak of probes. The superposition effect of tetracyclines and probes at 515 nm greatly improved the sensitivity of the ratiometric fluorescent sensor and widened the detection range, and linear ranges for oxytetracycline (OTC) and tetracycline (TC) were respectively 0.00–805.20 μM and 0.00–1039.50 μM. Moreover, the preparation procedure of the La-CDs was simple and time saving and the coupling agent was not required. A comparison of La-CDs with undoped carbon dots (un-CDs) showed that the optical performance and sensing performance of La-CDs were improved. In addition, a portable paper sensor with La-CDs as probes was preliminarily explored in this work, and the sensor has been applied to detect OTC and TC in pork and fish with satisfactory results.

Keywords Lanthanum-doped carbon dots · Ratiometric sensor · Tetracyclines · Inner filter effect

Introduction

Tetracyclines were an all-natural antibiotic that quickly suppressed bacterial growth. It worked by interfering with the synthesis of bacterial proteins and killed bacteria in very high concentrations [1]. Due to the merit of quickly suppressed bacterial growth, low cost, and growth promotion in animal breeding, tetracyclines have been widely used in livestock farms [2, 3]. However, the tetracyclines abuse for growth promotion in animal breeding has led to tetracyclines residues in animal products, which posed a serious threat to public health via food chains [4]. Recent researches show that long-term ingestion of tetracyclines from daily food, including meat, egg, milk, and honey, could cause harmful effects on physical health, such as anaphylaxis, gastrointestinal disturbance, hepatotoxicity, and yellowing of teeth [5, 6]. Among them, tetracyclines are more common in meat because they are commonly used in livestock farms to protect animals from the threat of diseases [2]. Therefore, many countries and organizations have stipulated the maximum residue limits for tetracyclines in meat [7, 8], for example, the maximum residue limit of tetracyclines in the muscle of all animal source foods is 100 μg kg^{-1} in China, the residue limit of tetracyclines in the muscle of poultry, cattle, and swine product is 100 μg kg^{-1} in European Union [9]. Therefore, it was very important and meaningful to monitor tetracyclines in meat.

Up to now, many of analytical methods have been employed for the detection of tetracyclines, including liquid chromatography-mass spectrometry [10], high-performance liquid chromatography [11], capillary electrophoresis [12], colorimetry [13], enzyme-linked immunosorbent assay [14], aptamer or antibody-based methods [15–17], chemiluminescence enzyme linked immunosorbent assay [18], and electrochemical sensors methods [19, 20]. However,

✉ Shi Gang Shen
shensg@hbu.edu.cn

✉ Jiang Xue Dong
dongjx@hbu.edu.cn

1   College of Chemistry and Environmental Science, Hebei University, Key Laboratory of Analytical Science and Technology of Hebei Province, Wusi Road, Baoding 071002, People's Republic of China

these analytical methods needed sophisticated instruments, specialized operators, costly biomolecular reagents, and time-consuming electrode modification or sample pretreatments. Nowadays, fluorescence methods have attracted to more and more attention due to rapid, facile, low cost, high efficiency, small sample dose demanded, simple operation, and real time. Therefore, the establishment of the fluorescence methods for tetracyclines detection was promising and meaningful. In recent years, many fluorescent materials were employed to detection tetracyclines, such as silicon quantum dots [21], molybdenum disulfide nanoplates [22], single metal–organic framework materia [23], metal nanoclusters [24], and carbon dots (CDs) [25–27]. CDs have drawn great attention owing to superior physical and chemical properties, including low toxicity, good biocompatibility, highly photoluminescent, and facile surface modification [5]. The metal-doped CDs can be synthesized by simple hydrothermal and widely used detection micromolecule, metal ion, and tetracyclines [28–30]. Compared to undoped CDs, the metal-doped CDs possess higher photoluminescence quantum yields and imparted novel functionalities, multicolor emission, enhanced antimicrobial activities, and so on [31, 32]. Therefore, it is an important approach to design and use metal-doped fluorescent CDs for developing tetracyclines sensors to improve sensing properties.

In addition, ratiometric fluorescent sensors have more merits than single signal responsive sensors. For example, the single signal sensors are susceptible to instrumental efficiency and environmental conditions, and ratiometric fluorescent sensors can decrease above interferences by selfcalibration [33]. So far, although some ratiometric fluorescent sensors have been reported to detect tetracyclines, the reported tetracyclines ratiometric fluorescent sensors are generally based on the probes after coupling europium ion; the sensing mechanism is attributed to target-induced inner filter effect (IFE) and fluorescence enhancement of europium ion. For example, Li and coworker reported a tetracycline sensor in the range of 0.01–60 μM with gold nanoclusters as probes based on IFE and the interaction of tetracycline and europium ion. Li and colleagues reported a ratiometric fluorescent sensor by Ir (III) complex-doped and europium-functionalized silicon nanoparticles as probes, and the tetracycline was detected in the range of 0.01–20 μM based on IFE and the interaction of tetracycline and europium ion; Ti and colleagues reported a ratiometric fluorescent sensor based on carboxylated graphitic carbon nitride nanosheets and Eu^{3+}, and the tetracycline was detected in the range of 10–40 μM. Furthermore, the reported ratio detection method for tetracycline possessed a narrow linear range, and the probe preparation was complicated and time-consuming [4, 34–36]. Moreover, tetracyclines possess a wide absorption band at around 220–430 nm [37, 38], when the excitation or emission band of the probes overlaps with the ultraviolet absorption of tetracyclines, the fluorescence of reaction system will quench, so a lot of probes can be used to detect tetracyclines by IFE, and it is a big challenge to design and develop ratiometric fluorescent sensor for tetracyclines detection. Therefore, it has a great theoretical and practical value to develop a new fluorescent probe with simple preparation method and establish tetracyclines sensors with a wide linear range.

According to literatures, lanthanum (La) could improve fluorescence and quantum yield of CDs. For example, Zhang et al. reported that a La loaded graphitic carbon nitride nanosheets, showing that the fluorescence intensity of La loaded graphitic carbon nitride nanosheets was enhanced compared with graphitic carbon nitride nanosheet [39]; Yang et al. reported that the fluorescence intensity and the quantum yield of CDs were improved after doping the La into CDs [40]. Therefore, La was selected as the doping element to obtain high-performance CDs in this work, and the La-CDs were prepared by hydrothermal method with citric acid (CA) and N,N′-Diethylthiourea as carbon source. Subsequently, the properties of La-CDs were investigated in detail, and further experiments showed that the La-CDs could be used as fluorescent probes to detect tetracyclines. Combining with the high pH-induced fluorescence enhancement of tetracyclines at 515 nm, a ratiometric fluorescent sensor for wide range detection of tetracyclines was established based on La-CDs as probes. A comparison of La-CDs with un-CDs showed that the optical performance and sensing performance of La-CDs were improved. The sensing mechanism was further explored in detail, attributing the fluorescence quenching to IFE coexisted with other quenching effect. The established sensor has been successfully applied on tetracyclines detection in meat. Moreover, this work provided a novel design thought of ratiometric fluorescent sensor and theory reference for developing new detection method of tetracyclines in foods.

Experimental section

Preparation of lanthanum-doped carbon dots

$La(NO_3)_3 \bullet 6H_2O$ (12.5 mM), CA (125 mM), and N,N′-Diethylthiourea (375 mM) were dissolved in 20-mL deionized water. After stirring for 10 min, the mixed solution was transferred to a 50-mL microwave digestion tank followed by hydrothermal treatment at 170 °C for 12 h; after cooling to room temperature, the La-CDs were obtained, and the La-CDs were diluted with 15-mL deionized water. To further purify La-CDs, the diluted resulting mixture was centrifuged at 12,000 rpm for 10 min and repeated three times to remove large or agglomerated particles. Finally, the obtained La-CDs solution was stored at

refrigerator (0–4 °C) for further use. The synthesis conditions of La-CDs was optimized and placed on the Supplementary Material (Fig. S1 and Fig. S2).

Detection of OTC and TC with ratiometric fluorescent sensor

Firstly, OTC (2.01 mM and 0.201 mM) or TC (2.08 mM and 0.208 mM) were freshly prepared. A series of OTC or TC solution with different volumes were added to 100 μL Britton-Robinson (BR, 0.04 M, pH = 12) buffer solution and different volumes of deionized water. Then, 5-μL La-CDs solution was added to the mixed solution, and the total volume was 1 mL. After incubation for 5 min at the room temperature, fluorescence spectra were recorded under the excitation wavelength of 370 nm. Moreover, the BR buffer solution was obtained by adding 0.02 M NaOH into the 0.04 M mixed acid solution (phosphoric acid, boric acid, and acetic acid) under the monitoring of pH meter.

Real sample preparation

Pork and fish were purchased from local market and treated according to the reported methods [41, 42] with small modification. Briefly, the skinless pork or fish (2.0 g) was smashed and then was immersed in acetonitrile/deionized water (V/V = 7/3, 5.0 mL). The mixture was homogenized by vortex for 3 min and sonicated for 15 min. Then, the pork or fish samples were centrifuged for 10 min at 5000 rpm to remove large particles. After centrifugal treatment, the solution was filtrated through

0.22-μm microporous membrane and diluted 25 times by using deionized water for detection.

Preparation of test paper

Firstly, 75 μL of La-CDs was mixed with 1.5 mL BR (0.04 M, pH = 12) buffer solution and deionized water, and the total volume was 15 mL. Then, filter paper of a suitable size was prepared and immersed into the above-mixed solution for 1 min. The filter paper was taken out and dried in 50 °C vacuum drying oven for 0.5 h to obtain the test paper. More detailed experimental information was shown in the Supplementary Material.

Results and discussion

Preparation and characterization of La-CDs

La-CDs were prepared by hydrothermal method, and the reaction vessels were microwave digestion tanks. Figure 1a shows the preparation schematic of the La-CDs, and the obtained La-CDs solution was transferred to a centrifuge tube and placed in freeze dryer. Then, the dried La-CDs were turned into thick solid and the photographs were obtained under visible light and UV light (Fig. 1b), indicating the thick solid was orange under visible light and emitted weak yellowish-green fluorescence in the aggregated state under UV light. The prepared La-CDs solution was diluted and the emission spectra were recorded by F-7000 fluorescence spectrophotometer, as shown in Fig. 1c, two maximum emissions were observed with the change of excitation wavelength from 280 to 420 nm, which was different from the fluorescence emission of excitation-dependent carbon dots [43], and the maximum emission wavelength of La-CDs

Fig. 1 a The schematic of the La-CDs preparation. **b** The photographs of the La-CDs solid under visible light (left) and UV light (right). **c** Fluorescence spectra of the diluted La-CDs under different excitations. **d** The ultraviolet absorption and fluorescence spectra of the La-CDs, insets were photographs of the diluted La-CDs solution under visible light (left) and UV light (right)
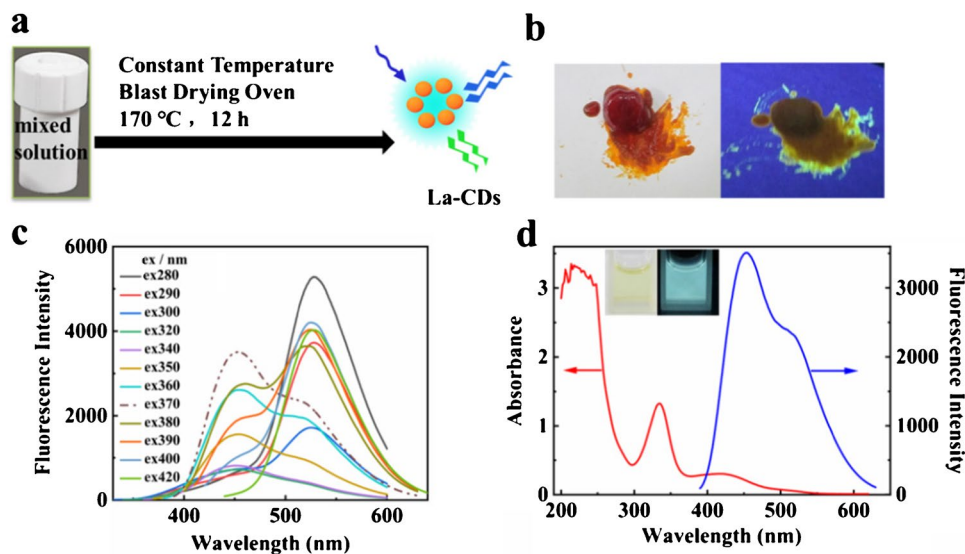
are located at 450 nm and 515 nm when the maximum excitation wavelengths are 370 nm and 280 nm, respectively. Figure 1d shows the ultraviolet absorption and fluorescence emission spectra of the La-CDs. The ultraviolet absorption spectrum of the La-CDs exhibited a wide absorption from 300 to 490 nm, which was attributable to the n-π* transition of La-CDs [26]. Furthermore, a sharp peak at 450 nm and a shoulder peak at 515 nm could be observed in fluorescence emission wavelength under an excitation wavelength of 370 nm, and the diluted La-CD water solution was pale yellow and emits blue-green fluorescence under UV light (inset of Fig. 1d).

The high-resolution transmission electron microscopy (HRTEM) images of the La-CDs displayed the morphology and size of the La-CDs, as shown in Fig. 2a and Fig. 2b; it could be observed that the La-CDs dispersed well with spherical shape, and the inset of Fig. 2a exhibits that the average diameter of the La-CDs was 5 nm. In addition, the hydrate particle size distribution of La-CDs was measured by dynamic light scattering (DLS) (Fig. S3). The mean hydrate particle size of La-CDs was 21.59 nm. The hydrate particle size was larger than the diameter measured by HRTEM. The reason was that the hydration particle size was given by DLS, including the particle nucleus and the surrounding solvated layer, while HRTEM only gave the diameter of the particle nucleus

[44]. The fourier-transform infrared (FT-IR) spectrum of La-CDs is shown in Fig. 2c, indicating that the O–H and N–H stretching vibration band at 3390 cm^{-1} can be observed [42], and the absorption at 1689 and 1646 cm^{-1} suggested the presence of C = N bending. Moreover, the asymmetric and symmetric stretching vibration of carboxylic groups (COO$^-$) can be observed at 1557 and 1410 cm^{-1}, respectively [45], and the absorptions in the region of 1000–1250 cm^{-1} were attributed to C-N [46]. The EDS spectrum showed that CDs were successfully modified by La^{3+} (Fig. 2d). Zeta (ζ) potential can be used to characterize the stability of colloid solutions. When the absolute value of ζ is > 30 mV, the colloid solution has good stability and the nanoparticles have good dispersibility [47]. The ζ potential of un-CDs (− 39.10 mV) and La-CDs (− 32.73 mV) were measured (Fig. 2e), indicating that the La-CDs and un-CDs have good thermodynamic stability. In addition, the ratio stability of the prepared La-CDs was further explored by detecting the change of the fluorescence intensity ratio (I_{515}/I_{450}) of prepared La-CDs solution with storage time; the results showed that the change of the I_{515}/I_{450} of La-CDs solution was less than 10% after 30 days at 4 °C in the refrigerator, as shown in Fig. S4, indicating that La-CDs could be stable at least one month at 4 °C in the refrigerator.
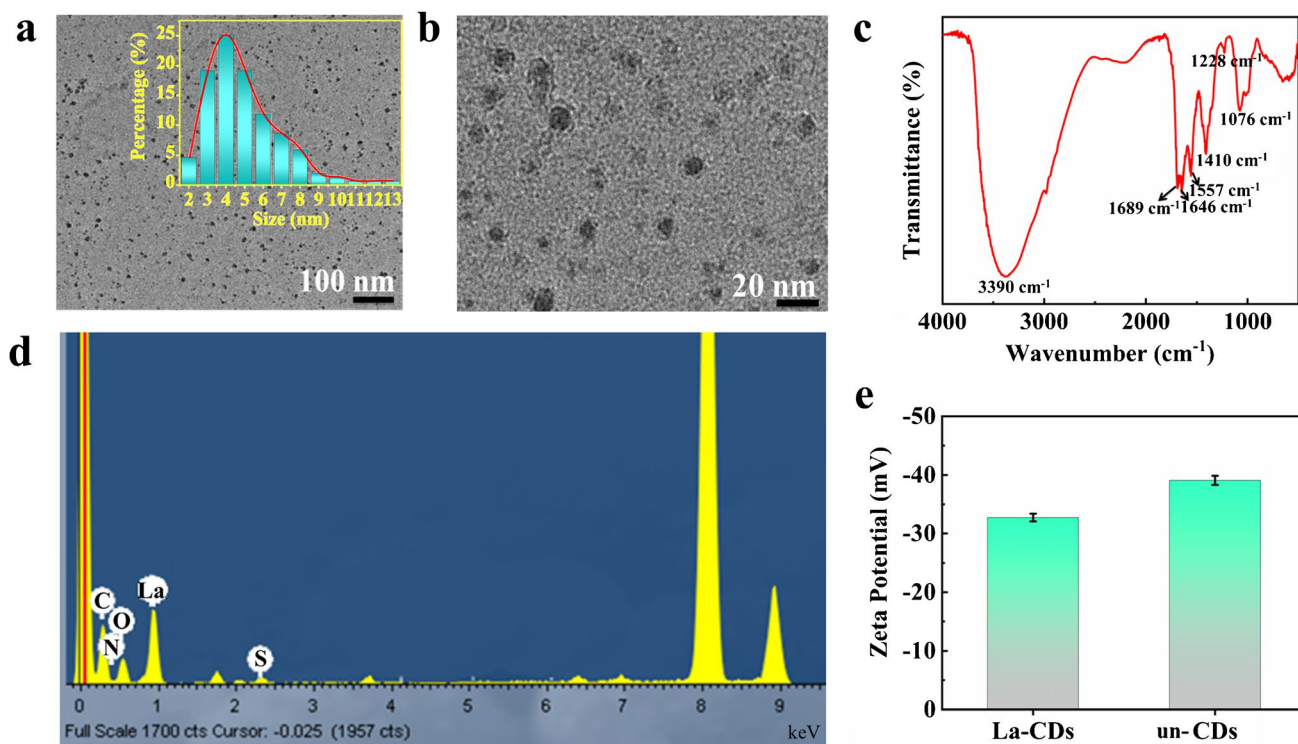

Fig. 2 **a** and **b** are the HRTEM images of La-CDs, the inset in (**a**) shows the size distribution of La-CDs. **c** FT-IR spectrum of La-CDs. **d** The EDS spectrum of La-CDs. **e** Zeta potential of La-CDs and un-CDs

Establishment of ratiometric fluorescent sensor

In this work, a fluorescence detection method of tetracyclines, OTC as the model, was developed based on the interaction between La-CDs and OTC. The analytical performance of the sensor was evaluated by the I_{515}/I_{450}. Figure 3a shows the fluorescent spectra of the La-CDs, La-CDs + OTC, and La-CDs + TC, respectively. When OTC or TC was added in the reaction system, the fluorescence of La-CDs was quenched and the value of I_{515}/I_{450} increased. Moreover, the detection conditions were investigated, such as the volume of La-CDs, pH, and reaction time. The dosage of probes was firstly explored, as shown in Fig. S5, the fluorescence intensity of emission spectrum decreased after the addition of 5-µL La-CDs; hence, 5-µL La-CDs was selected as the dosage of probes in this work. The pH was important to the detection system, in order to obtain preferable analytical performance, the effect of pH on sensor was explored and the results are shown in Fig. 3b, indicating that the I_{515}/I_{450} had little change of La-CDs in the absence of OTC when the pH increased from 4 to 12; however, the I_{515}/I_{450} of La-CDs in the presence of OTC gradually increased when the pH changed from 4 to 12. In order to understand why the I_{515}/I_{450} increases with the increase of pH, the fluorescence response of OTC was investigated under different pH values (pH 2–12), as shown in Fig. 3c, indicating that the fluorescence intensity at 515 nm gradually increased with the increase of pH. Therefore, pH 12 was selected to maintain the acidity of reaction system. The fluorescence of

tetracycline at 515 nm was significantly enhanced in alkaline solution, which had a superposition effect with the La-CDs at 515 nm, which significantly improved the value of I_{515}/I_{450}. Therefore, the pH-dependence of tetracyclines made a great contribution to the construction of the ratio sensor. In addition, the reaction time was studied; Fig. 3d shows that the reaction between La-CDs and OTC was fast and could be completed in 5 min, and the results indicated that La-CDs and La-CDs + OTC could keep stable for at least 120 min.

Sensitivity of sensor

Under the optimal conditions, the sensitivity of established sensor was explored for the quantitative detection of OTC and TC in aqueous solution. Figure 4a and Fig. 4c were the fluorescence spectra of the reaction system in the presence of various concentrations of OTC and TC. As shown in Fig. 4b and Fig. 4d, the I_{515}/I_{450} had a good linear relationship to OTC and TC concentrations in the range of 0.00–805.20 µM and 0.00–1039.50 µM, respectively. The linear equations for OTC and TC detection were respectively $I_{515}/I_{450} = 0.007 \, [\text{OTC}] + 0.6596$ ($R = 0.9986$) and $I_{515}/I_{450} = 0.0036 \, [\text{TC}] + 0.5884$ ($R = 0.9936$), and the corresponding limit of detection (LOD) were 42.90 nM and 83.30 nM, respectively. Figure 4e and Fig. 4f are the corresponding CIE chromaticity diagrams of the La-CDs in the presence of various concentrations of OTC and TC, respectively. Figure 4g and Fig. 4h are the corresponding photographs for OTC and TC detection under UV light (365 nm),

Fig. 3 **a** Fluorescence spectra of the La-CDs (curve 1), La-CDs + OTC (curve 2), and La-CDs + TC(curve 3), respectively. **b** The change of I_{515}/I_{450} of La-CDs and La-CDs + OTC with the pH. **c** Fluorescence spectra of OTC with different of pH (BR, 0.04 M). **d** The I_{515}/I_{450} change of La-CDs and La-CDs + OTC with the time
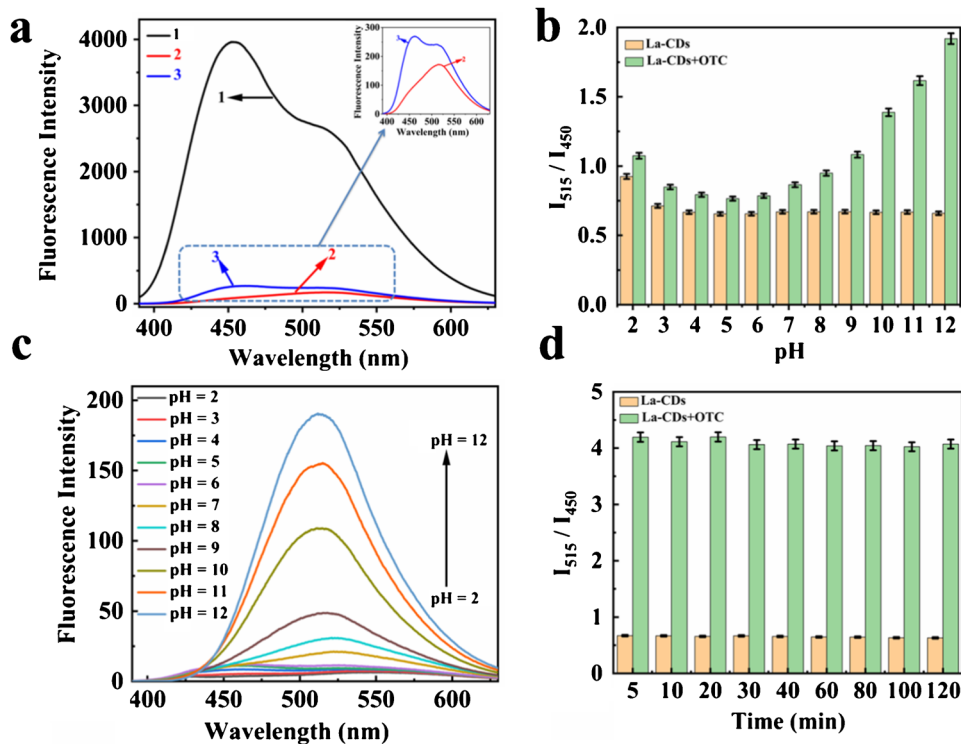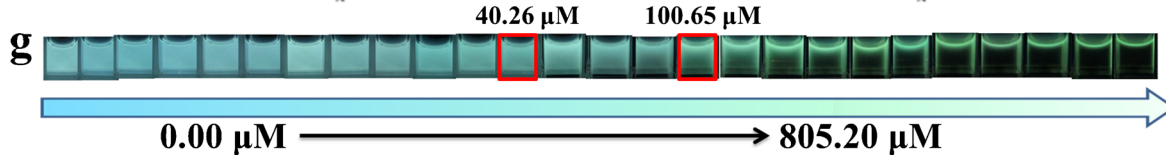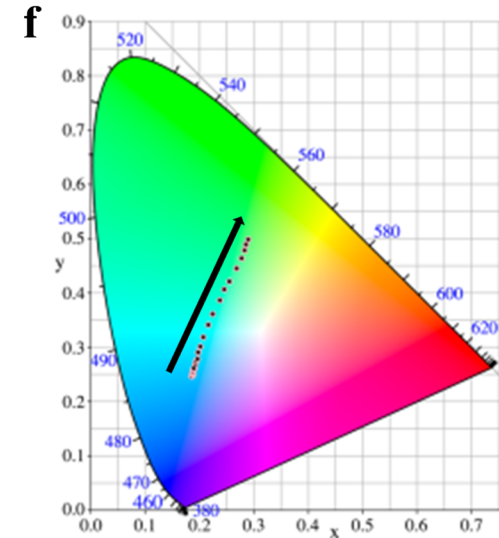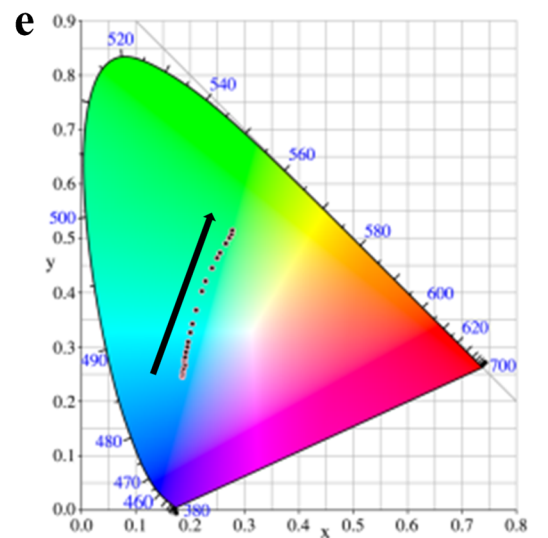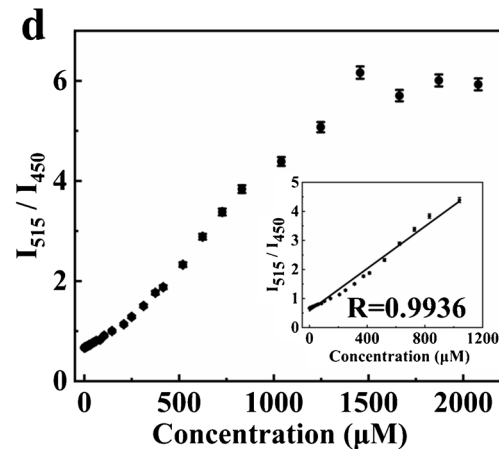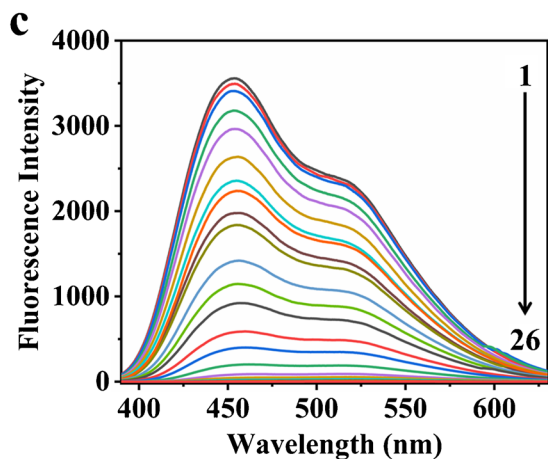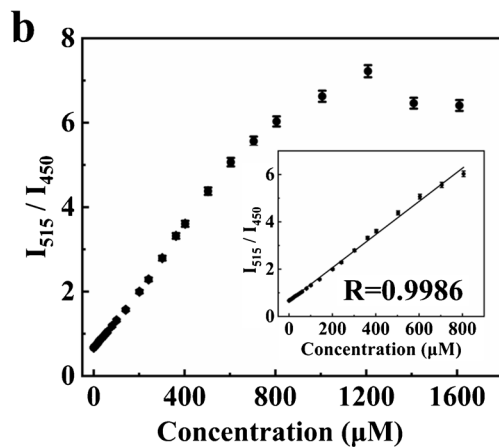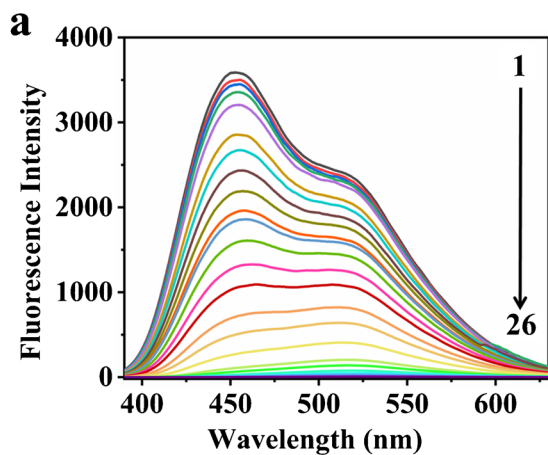
◄**Fig. 4 a** and **c** were fluorescence spectra of the reaction system in the presence of various concentrations of OTC (number 1–26: 0.00, 0.20, 0.60, 2.01, 6.04, 10.07, 14.09, 18.12, 22.14, 26.17, 30.20, 40.26, 50.33, 60.39, 80.52, 100.65, 140.91, 201.30, 241.56, 301.95, 362.34, 402.60, 503.25, 603.90, 704.55, 805.20 μM) and TC (number 1–26: 0.00, 0.21, 2.08, 6.24, 10.40, 14.55, 18.71, 22.87, 27.03, 31.19, 41.58, 51.98, 62.37, 83.16, 103.95, 145.50, 207.90, 249.48, 311.85, 374.22, 415.80, 519.75, 623.70, 727.65, 831.60, 1039.50 μM), respectively. **b** and **d** are the plots of the I_{515}/I_{450} versus the concentration of OTC and TC, respectively, insets show the corresponding linear response regions for OTC and TC. **e** and **f** the corresponding CIE chromaticity diagram of the La-CDs in the presence of corresponding concentration of OTC and TC, respectively. **g** and **h** are the corresponding photographs of the La-CDs solution in various concentrations of OTC and TC under UV light, respectively

respectively. The CIE chromaticity diagram and photographs for OTC and TC detection under UV light indicated that the established ratiometric fluorescent sensor could distinguish the OTC or TC concentration by fluorescent color variation.

Moreover, the un-CDs were prepared at the same experimental conditions with La-CDs, and the fluorescence property and sensor performance of the un-CDs for detection of OTC were compared with La-CDs. The results showed that the fluorescence intensity of La-CDs (Fig. 4a) greatly enhanced compared with the un-CDs at the same concentration of probes (Fig. S6a), and the fluorescence quantum yield (QY) of La-CDs (QY = 11.68%) increased compared with the un-CDs (QY = 9.44%) using quinine sulfate as a reference. The measurement method of QY was placed in the Supplementary Material. At the same time, the fluorescence intensity of un-CDs progressively decreased with the increased concentration of OTC (Fig. S6a). The linear relationship (R = 0.9980) between the I_{515}/I_{450} and OTC concentration was obtained ranging from 2.01 to 603.90 μM. The linear equation for OTC detection was $I_{515}/I_{450} = 0.0074$ [OTC] + 0.4473 (Fig. S6b). For La-CDs, the I_{515}/I_{450} had a good linear relationship to OTC concentrations in the range of 0.00–805.20 μM (Fig. 4b). As a comparison, La-CDs had the wider linear range and higher sensitivity.

In addition, as shown in Table S1, the established tetracyclines sensor in this work possesses wide detection range, and the recovery and relative standard deviation (RSD) are comparable to the reported ratiometric methods.

Selectivity of sensor

These effects of some potential interfering substances that existed in real samples for OTC and TC detection were investigated in this work under experiment conditions, including the various small molecules and common ionic. Figure 5 shows the I_{515}/I_{450} of reaction system with various small molecules and common ionic, indicating that most of small molecules and common ionic had little effect on the OTC and TC detection under experiment conditions,

and the established sensor has good selectivity for OTC and TC. The results of selectivity experiments indicated that the sensor had a certain practical application value for the selective analysis of OTC and TC in real samples. The concentration of L-Cysteine (L-Cys), thiamine (VB1), vitamin B6 (VB6), L-histamine (L-His), L-glutamine (L-Glu), L-glutathione (L-GSH), phenylalanine (L-Phe), L-tyrosine (L-Tyr), D-(+)-glucose (D-(+)-Glc), chloramphenicol (Chl), CA, PO_4^{2-}, CO_3^{2-}, HCO_3^-, F^-, SO_4^{2-}, Cl^-, NO_3^-, Ac^-, $C_2O_4^{2-}$, Na^+, Ca^{2+}, Mg^{2+}, K^+, Zn^{2+}, Al^{3+}, Cu^{2+}, and Ni^{2+} was 10.4 mM, the concentration of erythromycin (Ery) was 2.08 mM, and the concentration of L(+)-ascorbic acid (L(+)-VC) and Fe^{3+} was 1.04 mM.

Sensing mechanism

Moreover, the sensing mechanism for tetracyclines detection has been explored in this work, and OTC was selected as the representative substance of tetracyclines for the following experiments. As shown in Fig. 4g, when the concentrations of OTC were 40.26 μM, the fluorescence quenching was not obvious under UV light; when the concentrations of OTC were 100.65 μM, the fluorescence quenching was remarkable under UV light, and the fluorescence color changed from blue to green. Hence, the above two concentrations of OTC (40.26 and 100.65 μM) were selected as representative of low and high concentrations of OTC, respectively, and the mechanism was explored by measuring the fluorescence lifetime of reaction solutions containing the above two concentrations of OTC. The fluorescence quenching of La-CDs was described by the Stern–Volmer plot following the equation [22]:

$I_0 (450)/I (450) = K_{sv}C_q + 1 = K_q\tau_0 C_q + 1$ (E 1) where $I_0 (450)$ and $I (450)$ were the fluorescence intensity of La-CDs in the absence and in the presence of OTC at 450 nm, respectively; C_q was the concentration of OTC; K_{sv} was the quenching constant at emission wavelength (450 nm) and calculated to be 0.0331 $μM^{-1}$ (Fig. S7a). τ_0 was the fluorescence lifetime of La-CDs, K_q was quenching rate constant and calculated to be 4.1×10^{12} M^{-1} s^{-1}, far greater than 2×10^{10} M^{-1} s^{-1} according to E 1, indicating the static quenching dominated in low concentration of OTC (40.26 μM). The relationship between $I_0 (450)/I (450)$ and high concentration of OTC (100.65 μM) were upward curvature (Fig. S7b), indicating the dynamic quenching coexisted with the static quenching [22, 48] in presence of high concentration of OTC. As shown in Fig. 6a, in the absence of OTC and presence of OTC (40.26 μM and 100.65 μM), the fluorescence lifetime was 8.05 ns, 7.85 ns, and 4.41 ns, respectively. The fluorescence lifetimes showed that the static quenching dominated in low concentration of OTC and the dynamic quenching coexisted with the static quenching in high concentration of OTC [49, 50].
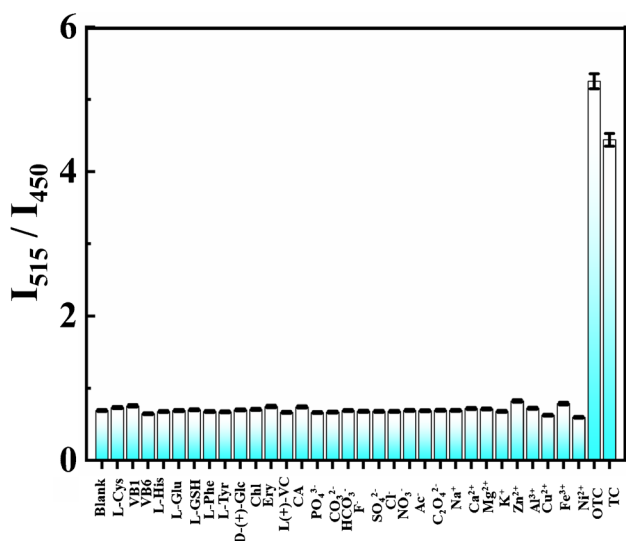
Fig. 5 Selectivity of ratiometric sensor in the presence of various small molecules and common ionic

Figure 6b displayed the ultraviolet absorption spectra of La-CDs, La-CDs + OTC, and OTC, showing that the La-CDs and OTC displayed the wide absorption band at around 280–470 nm and 220–430 nm, respectively, which indicated that the ultraviolet absorption spectra of La-CDs and OTC overlapped. Moreover, the ultraviolet absorption spectrum of La-CDs + OTC was the additive result of the ultraviolet absorption spectra of La-CDs and OTC, illustrating that no new chemical substance was formed in the interaction between La-CDs and OTC. Combining with the change of the fluorescence lifetime, therefore, the tetracyclines sensor mechanism was considered to be the IFE [50]. In order to further confirm that the IFE was responsible for the tetracyclines sensing mechanism, a related correction was performed using equation E S1 (Equation E S1 was placed in the Supplementary Material). Fig. S8 and Table S2 show the relevant data and results. When CF ≤ 3, the fluorescence quenching was attributed to the IFE; when CF > 3,

the fluorescence quenching was attributed to IFE and other quenching mechanism [49, 51]. The fluorescence quenching efficiency before and after correction of OTC toward La-CDs is shown in Fig. S9. The result showed that the fluorescence quenching of La-CDs was caused by IFE in low concentration of OTC. The fluorescence quenching of La-CDs might be caused by IFE and other quenching mechanism in high concentration of OTC. Therefore, the sensing mechanism of proposed tetracyclines sensor was attributed to IFE and the static quenching effect in low concentration of OTC, IFE, and the dynamic quenching coexisted with the static quenching in high concentration of OTC.

Application of sensor

In order to explore the practical application value of the established sensor for OTC and TC detection, the standard addition methods were employed to measure OTC and TC levels in pork and fish samples. The analytical results are shown in Table S3, and the recovery values were 90.08–114.90% with RSD of 0.13–2.78%. The above results were receivable for the quantitative analysis of OTC and TC in real samples and showed that the established sensor has been successfully applied to detect OTC and TC in real samples. In addition, the La-CD solutions were employed to prepare the test papers in this work. Figure 7a shows the prepared test papers by our laboratory. The OTC and TC solutions were dipped and wrote "HBU" on the test papers, as shown in Fig. 7b, indicating that the established tetracyclines sensor is promising to develop portable paper sensor for visual tetracyclines detection.

Conclusions

In summary, La-CDs were prepared by hydrothermal with good water solubility and stability in this work, and the La-CDs were employed to develop a ratiometric fluorescent sensor for tetracyclines detection combining the pH-dependence

Fig. 6 **a** The fluorescence lifetime measurement of La-CDs and La-CDs + OTC. **b** The ultraviolet absorption spectra of La-CDs, La-CDs + OTC, and OTC
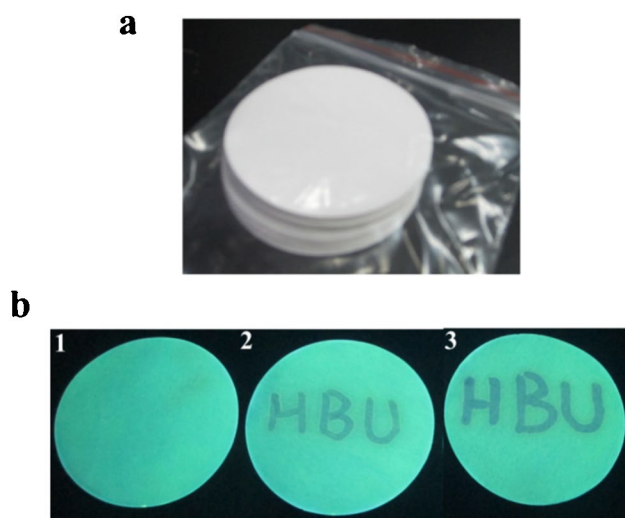
a

b
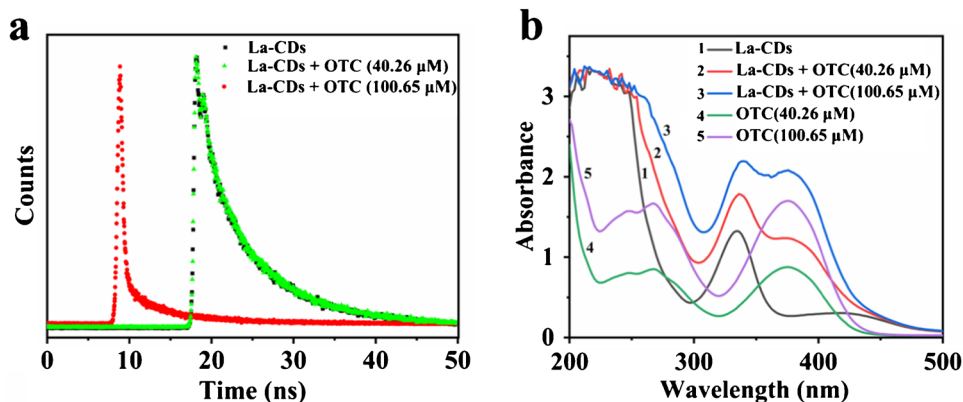
Fig. 7 **a** Photograph of the test paper was prepared by our laboratory in this work. **b** Photographs of the results of test papers under UV light, no. 1 shows the blank test paper, nos. 2 and 3 show the test papers that were dipped with OTC and TC solutions and wrote "HBU," respectively

of targets; the sensing mechanism has been discussed and attributed to IFE and other quenching effect. A comparison of La-CDs with un-CDs showed that La-CDs had wider linear range and higher sensitivity, and the sensor has been successfully applied to detect tetracyclines in meat. In addition, a portable paper sensor with La-CDs as probes was preliminarily explored in this work, and the results were satisfactory. These indicated that La-CDs have great application prospect in the field of constructing tetracycline sensor and portable paper.

Declarations

Conflict of interest The authors declare no competing interests.

References

1. Li RX, Wang WJ, El-Sayed E-SM, Su KZ, He PL, Yuan DQ. Ratiometric fluorescence detection of tetracycline antibiotic based on a polynuclear lanthanide metal–organic framework. Sensor Actuat B: Chem. 2021;330:129314.
2. Sreejith S, Shajahan S, Prathiush PR, Anjana VM, Viswanathan A, Chandran V, et al. Healthy broilers disseminate antibiotic resistance in response to tetracycline input in feed concentrates. Microb Pathogensis. 2020;149:104562.
3. Wei W, He J, Wang YY, Kong MJ. Ratiometric method based on silicon nanodots and Eu(3+) system for highly-sensitive detection of tetracyclines. Talanta. 2019;204:491–8.
4. Li YY, Du QQ, Zhang XD, Huang YM. Ratiometric detection of tetracycline based on gold nanocluster enhanced Eu(3+) fluorescence. Talanta. 2020;206:120202.
5. Li L, Shi LH, Jia J, Eltayeb O, Lu WJ, Tang YH, et al. Red fluorescent carbon dots for tetracycline antibiotics and pH discrimination from aggregation-induced emission mechanism. Sensor Actuat B: Chem. 2021;332:129513.
6. Xu J, Shen XK, Jia L, Zhou TL, Ma TL, Xu ZQ, et al. A novel visual ratiometric fluorescent sensing platform for highly-sensitive visual detection of tetracyclines by a lanthanide- functionalized palygorskite nanomaterial. J Hazard Mater. 2018;342:158–65.
7. Han S, Yang L, Wen ZG, Chu SY, Wang M, Wang ZY, et al. A dual-response ratiometric fluorescent sensor by europium-doped CdTe quantum dots for visual and colorimetric detection of tetracycline. J Hazard Mater. 2020;398:122894.
8. Wu ZT, Zhou Y, Huang HY, Su Z, Chen SM, Rong MC. BCNO QDs and ROS synergistic oxidation effect on fluorescence enhancement sensing of tetracycline. Sensor Actuat B: Chem. 2021;332:129530.
9. Perez-Rodriguez M, Pellerano RG, Pezza L, Pezza HR. An overview of the main foodstuff sample preparation technologies for tetracycline residue determination. Talanta. 2018;182:1–21.
10. Aguilera-Luiz MM, Vidal JL, Romero-Gonzalez R, Frenich AG. Multi-residue determination of veterinary drugs in milk by ultra-high-pressure liquid chromatography-tandem mass spectrometry. J Chromatogr A. 2008;1205(1–2):10–6.
11. Feng MX, Wang GN, Yang K, Liu HZ, Wang JP. Molecularly imprinted polymer-high performance liquid chromatography for the determination of tetracycline drugs in animal derived foods. Food Control. 2016;69:171–6.
12. Ibarra IS, Rodriguez JA, Miranda JM, Vega M, Barrado E. Magnetic solid phase extraction based on phenyl silica adsorbent for the determination of tetracyclines in milk samples by capillary electrophoresis. J Chromatogr A. 2011;1218(16):2196–202.
13. Tang Y, Huang XH, Wang XL, Wang CX, Tao H, Wu YG. G-quadruplex DNAzyme as peroxidase mimetic in a colorimetric biosensor for ultrasensitive and selective detection of trace tetracyclines in foods. Food Chem. 2021;366:130560.
14. Diana S. Aga RGaPK. Application of ELISA in determining the fate of tetracyclines in land-applied livestock wastes. Analyst. 2003;128:658–62.
15. Ahmed SR, Kumar S, Ortega GA, Srinivasan S, Rajabzadeh AR. Target specific aptamer-induced self-assembly of fluorescent graphene quantum dots on palladium nanoparticles for sensitive detection of tetracycline in raw milk. Food Chem. 2021;346:128893.
16. Wang S, Dong YY, Liang X. Development of a SPR aptasensor containing oriented aptamer for direct capture and detection of tetracycline in multiple honey samples. Biosens Bioelectron. 2018;109:1–7.
17. Zhang L, Wang JP, Deng JK, Wang S. A novel fluorescent "turn-on" aptasensor based on nitrogen-doped graphene quantum dots and hexagonal cobalt oxyhydroxide nanoflakes to detect tetracycline. Anal Bioanal Chem. 2020;412(6):1343–51.
18. Wang G, Zhang HC, Liu J, Wang JP. A receptor-based chemiluminescence enzyme linked immunosorbent assay for determination of tetracyclines in milk. Anal Biochem. 2019;564–565:40–6.

19. Jin L, Qiao JT, Chen JH, Xu N, Wu MS. Combination of area controllable sensing surface and bipolar electrode-electrochemiluminescence approach for the detection of tetracycline. Talanta. 2020;208:120404.

20. Taghdisi SM, Danesh NM, Ramezani M, Abnous K. A novel M-shape electrochemical aptasensor for ultrasensitive detection of tetracyclines. Biosens Bioelectron. 2016;85:509–14.

21. Zhang L, Wang YL, Jia L, Bi N, Bie HY, Chen XZ, et al. Ultrasensitive and visual detection of tetracycline based on dual-recognition units constructed multicolor fluorescent nano-probe. J Hazard Mater. 2021;409:124935.

22. Jia P, Bu T, Sun XY, Liu YG, Liu JH, Wang QZ, et al. A sensitive and selective approach for detection of tetracyclines using fluorescent molybdenum disulfide nanoplates. Food Chem. 2019;297:124969.

23. Xiong J, Yang L, Gao LX, Zhu PP, Chen Q, Tan KJ. A highly fluorescent lanthanide metal-organic framework as dual-mode visual sensor for berberine hydrochloride and tetracycline. Anal Bioanal Chem. 2019;411(23):5963–73.

24. Khataee A, Jalili R, Dastborhan M, Karimi A, Ebadi Fard Azar A. Ratiometric visual detection of tetracycline residues in milk by framework-enhanced fluorescence of gold and copper nanoclusters. Spectrochim Acta A. 2020;242:118715.

25. Fu Q, Long CC, Qin LF, Jiang ZX, Qing TP, Zhang P, et al. Fluorescent and colorimetric dual-mode detection of tetracycline in wastewater based on heteroatoms-doped reduced state carbon dots. Environ Pollut. 2021;283:117109.

26. Zhao CX, Jiao Y, Gao Z, Yang YL, Li H. N, S co-doped carbon dots for temperature probe and the detection of tetracycline based on the inner filter effect. J Photoch Photobio A. 2018;367:137–44.

27. Wu L, Long R, Li T, Tang C, Tong X, Guo Y, et al. One-pot fabrication of dual-emission and single-emission biomass carbon dots for Cu(2+) and tetracycline sensing and multicolor cellular imaging. Anal Bioanal Chem. 2020;412(27):7481–9.

28. Guo JH, Lu WJ, Zhang HL, Meng YT, Du FF, Shuang SM, et al. Copper doped carbon dots as the multi-functional fluorescent sensing platform for tetracyclines and pH. Sensor Actuat B: Chem. 2021;330:129360.

29. Ma YS, Cen Y, Sohail M, Xu GH, Wei FD, Shi ML, et al. A ratiometric fluorescence universal platform based on N, Cu codoped carbon dots to detect metabolites participating in H_2O_2-generation reactions. ACS Appl Mater Inter. 2017;9(38):33011–9.

30. Zhang M, Wang WT, Zhang J, Zhou NL. Synthesis of lanthanum doped carbon dots for detection of mercury ion, multi-color imaging of cells and tissue, and bacteriostasis. Chem Eng J. 2017;330:1137–47.

31. Xu Q, Su RG, Chen YS, Theruvakkattil Sreenivasan S, Li N, Zheng XS, et al. Metal charge transfer doped carbon dots with reversibly switchable, ultra-High quantum yield photoluminescence. ACS Applied Nano Mater. 2018;1(4):1886–93.

32. Tejwan N, Saini AK, Sharma A, Singh TA, Kumar N, Das J. Metal-doped and hybrid carbon dots: a comprehensive review on their synthesis and biomedical applications. J Control Release. 2021;330:132–50.

33. Wang YH, Zhang C, Chen XC, Yang B, Yang L, Jiang CL, et al. Ratiometric fluorescent paper sensor utilizing hybrid carbon dots-quantum dots for the visual determination of copper ions. Nanoscale. 2016;8(11):5977–84.

34. Li XT, Fan KM, Yang RM, Du XX, Qu BH, Miao XM, et al. A long lifetime ratiometrically luminescent tetracycline nanoprobe based on Ir(III) complex-doped and Eu(3+)-functionalized silicon nanoparticles. J Hazard Mater. 2020;386:121929.

35. Ti MR, Li YS, Li ZQ, Zhao DX, Wu L, Yuan LF, et al. A ratiometric nanoprobe based on carboxylated graphitic carbon nitride nanosheets and Eu(3+) for the detection of tetracyclines. Analyst. 2021;146(3):1065–73.

36. Wu WJ, Zhao Q, Zhou R, Liang YC, Zhao WB, Shan CX. Ratiometric fluorescence sensor based on europium-grafted ZnO quantum dots for visual and colorimetric detection of tetracycline. Spectrochim Acta A. 2021;259:119901.

37. Li MT, Zhu NW, Zhu W, Zhang SH, Li F, Wu PX, et al. Enhanced emission and higher stability ovalbumin-stabilized gold nanoclusters (OVA-AuNCs) modified by polyethyleneimine for the fluorescence detection of tetracyclines. Microchem J. 2021;169:106560.

38. Li CL, Zeng CH, Chen Z, Jiang YF, Yao H, Yang YY, et al. Luminescent lanthanide metal-organic framework test strip for immediate detection of tetracycline antibiotics in water. J Hazard Mater. 2020;384:121498.

39. Zhang HQ, Huang YH, Lin XH, Lu FF, Zhang ZS, Hu ZB. Lanthanum loaded graphitic carbon nitride nanosheets for highly sensitive and selective fluorescent detection of iron ions. Sensor Actuat B: Chem. 2018;255:2218–22.

40. Yang SH, Sun XH, Wang ZY, Wang XY, Guo GS, Pu QS. Anomalous enhancement of fluorescence of carbon dots through lanthanum doping and potential application in intracellular imaging of ferric ion. Nano Res. 2018;11(3):1369–78.

41. Lin BX, Zhang TY, Xin XL, Wu D, Huang Y, Liu YW, et al. Europium(III) modified silicone nanoparticles for ultrasensitive visual determination of tetracyclines by employing a fluorescence color switch. Microchim Acta. 2019;186(7):442.

42. Xing XJ, Huang L, Zhao SJ, Xiao JF, Lan MH. S,N-Doped carbon dots for tetracyclines sensing with a fluorometric spectral response. Microchem J. 2020;157.

43. Liu SG, Liu T, Li N, Geng S, Lei JL, Li NB, et al. Polyethylenimine-derived fluorescent nonconjugated polymer dots with reversible dual-signal pH response and logic gate operation. J of Phys Chem C. 2017;121(12):6874–83.

44. Han L, Liu SG, Zhang XF, Tao BX, Li NB, Luo HQ. A sensitive polymer dots-manganese dioxide fluorescent nanosensor for "turn-on" detection of glutathione in human serum. Sensor Actuat B: Chem. 2018;258:25–31.

45. Yang Y, Wei QY, Zou T, Kong YL, Su LF, Ma D, et al. Dual-emission ratiometric fluorescent detection of dinotefuran based on sulfur-doped carbon quantum dots and copper nanocluster hybrid. Sensor Actuat B: Chem. 2020;321:128534.

46. Zhang X, Tan XY, Hu YP. Blue/yellow emissive carbon dots coupled with curcumin: a hybrid sensor toward fluorescence turn-on detection of fluoride ion. J Hazard Mater. 2021;411:125184.

47. Dong JX, Gao ZF, Zhang Y, Li BL, Zhang W, Lei JL, et al. The pH-switchable agglomeration and dispersion behavior of fluorescent Ag nanoclusters and its applications in urea and glucose biosensing. NPG Asia Mater. 2016;8(12):e335-e.

48. Lin M, Zou HY, Yang T, Liu ZX, Liu H, Huang CZ. An inner filter effect based sensor of tetracycline hydrochloride as developed by loading photoluminescent carbon nanodots in the electrospun nanofibers. Nanoscale. 2016;8(5):2999–3007.

49. Yan FY, Sun ZH, Pang JP, Jiang YX, Zheng WX. Functionalized carbon dots of thiazole derivatives based on inner filter effect for tetracyclines detection. Dyes Pigments. 2020;183:108673.

50. Zhang Y, Lv M, Gao PF, Zhang GM, Shi LH, Yuan MJ, et al. The synthesis of high bright silver nanoclusters with aggregation-induced emission for detection of tetracycline. Sensor Actuat B: Chem. 2021;326:129009.

51. Han L, Fan YZ, Qing M, Liu SG, Yang YZ, Li NB, et al. Smartphones and test paper-assisted ratiometric fluorescent sensors for semi-quantitative and visual assay of tetracycline based on the target-induced synergistic effect of antenna effect and inner filter effect. ACS Appl Mater Interfaces. 2020;12(41):47099–107.